

¹²Bismarck-Nasr, M. N., "Supersonic Panel Flutter Analysis of Shallow Shells," *AIAA Journal*, Vol. 31, No. 7, 1993, pp. 1349–1351.

¹³Bismarck-Nasr, M. N., "Dynamic Stability of Shallow Shells Subjected to Follower Forces," *AIAA Journal*, Vol. 33, No. 2, 1995, pp. 355–360.

¹⁴Bismarck-Nasr, M. N., "Aeroelasticity of Laminated Fibre-Reinforced Doubly Curved Shallow Shells," *AIAA Journal*, Vol. 36, No. 4, 1998, pp. 661–663.

¹⁵Reissner, E., and Stavsky, Y., "Bending and Stretching of Certain Types of Heterogeneous Anisotropic Elastic Plates," *Journal of Applied Mechanics*, Vol. 26, No. 9, 1961, pp. 402–408.

¹⁶Jones, R. M., *Mechanics of Composite Materials*, McGraw-Hill—Kogakusha Ltd., Tokyo, 1975.

Aeroelastic Design Optimization with Experimental Verification

Jakob Kutenkeuler* and Ulf Ringertz†
Royal Institute of Technology,
Stockholm S-100 44, Sweden

Introduction

THE optimal design of aircraft structures subject to aeroelastic stability constraints, so-called aeroelastic tailoring, is not new. Early studies involved using the anisotropic properties of laminated wood or plywood structures to tailor the structural response caused by aerodynamic forces.¹ The development of finite element structural analysis, potential flow panel methods, and numerical optimization made it possible to solve quite complex aeroelastic tailoring problems. Important early contributions were done by Haftka and Yates² and Wilkinson et al.³ Use of modern composite materials have further improved the possibilities in tailoring the structural response under aerodynamic loads for performance benefits. The X-29 demonstrator is perhaps the most well-known example.⁴

Because aeroelastic tailoring is true multidisciplinary analysis and optimization, there is an obvious risk that modeling errors in each discipline multiply when the different models are combined in an optimization process. Evaluation of the aeroelastic stability constraints involves the solution of nonlinear eigenvalue problems with unsymmetric and complex matrices. It is well known that this type of eigenvalue constraint is not differentiable with respect to design changes and may also lead to discontinuities in other problem parameters such as flutter speed.^{5–7}

The purpose of the present paper is to demonstrate the accuracy of the most common analysis methods used in aeroelastic tailoring for predicting aeroelastic stability by comparing numerical results with wind-tunnel experiments. The particular interest is to closely investigate design points in the neighborhood of optimal designs where discontinuities in flutter speed with respect to design changes appear. The use of optimal design methods tends to increase the likelihood of obtaining structures that, at least in theory, are extremely sensitive to small perturbations and imperfections in material properties, boundary conditions, and aerodynamic flow models.

Model Problem

The model design problem was chosen as a thin composite wing with orthotropic material properties. The design variables

Received Jan. 15, 1997; revision received Nov. 15, 1997; accepted for publication Jan. 9, 1998. Copyright © 1998 by the American Institute of Aeronautics and Astronautics, Inc. All rights reserved.

*Ph.D. Student, Department of Aeronautics. E-mail: jakob@flyg.kth.se.

†Professor, Department of Aeronautics. E-mail: rzu@flyg.kth.se. Member AIAA.

were the orientation of the material and the size of a number of concentrated masses used for mass balancing. There are several advantages with using a polymer composite wing. The composite material is superior in withstanding large strains, e.g., when subject to flutter, without permanent deformations caused by yielding and it offers many possibilities for aeroelastic tailoring.

The wing geometry and material were selected on the basis of tunnel performance and geometry. The configuration was chosen to be of relevant size, materialize a suitable critical speed, and to not have a divergence instability. A 15-deg swept configuration with 1200-mm span, 200-mm root chord, and 100-mm tip chord was chosen. Planform and definition of the coordinate system are shown in Fig. 1, where γ defines the sweep angle and θ defines the orientation of the 0-deg laminate axis. The nominal wing thickness was 2.0 mm.

All wings were cut from prefabricated, epoxy-impregnated woven glass-fiber laminates with the objective to be identical with respect to planform and thickness. The lay-up was orthotropic with all fibers aligned parallel to either the 0- or 90-deg axis of the laminate. Because of differences in the weave structure between the warp and weft yarns, both the Young's moduli and the bending stiffnesses varied between the two main axes. The 0-deg axis was defined here as the axis of highest stiffness.

The dominating elastic material properties in the present aeroelastic problem are the plate stiffnesses, D_{ij} . Several different mechanical tests were performed to determine reliable and representative material properties. After some consideration it was decided to consistently use the results from a vibration technique^{8,9} that is able to measure all D_{ij} of a specimen in one single test. The advantage of the method was notable, particularly because it is quite difficult to measure, e.g., D_{66} using standard test methods.

The method of Frederiksen^{8,9} uses experimentally determined eigenfrequencies of rectangular specimen plates to match numerical results where the elastic lamina properties are used as variables in an optimization process. An error function describing the difference between the experiments and the numerical results is minimized. The experiments showed variations in elastic properties, primarily because of laminate thickness variations, but likely also because of local deviations in lamina orientations. Table 1 shows representative plate stiffnesses for the thinnest, average, and thickest wing in the investigation. All material data are given in the global x - y coordinate system defined in Fig. 1.

The out-of-plane shear moduli G_{13} and G_{23} were also needed because the Mindlin plate differential equations¹⁰ were used in

Table 1 Representative material properties for the glass-fiber/epoxy laminates

Thickness, mm	Density, kg/m ³	D_{11} , Nm	D_{22} , Nm	D_{12} , Nm	D_{66} , Nm
1.95	1978	18.1	16.4	2.84	3.76
2.06	1929	20.0	18.2	3.19	4.23
2.14	1916	21.8	19.5	3.31	4.48

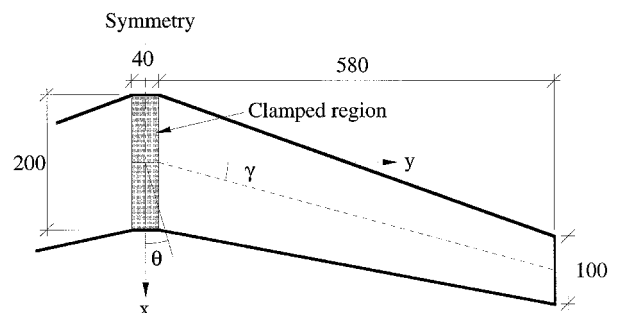


Fig. 1 Wing geometry and coordinate system.

the structural model. A single test was used to estimate these moduli giving $G_{13} = 4.27$ GPa and $G_{23} = 3.56$ GPa. These results were used throughout the analyses because their effect on stiffness is negligible because of the small thickness of all laminates used.

Numerical Analysis

The linearized equations of motion for a thin wing in potential flow are given in discretized form as

$$M\ddot{\mathbf{v}} + K\mathbf{v} = \mathbf{f}(t) \quad (1)$$

where the vector \mathbf{v} denotes the nodal displacements of the wing finite element model, M , the consistent mass matrix, K , the stiffness matrix, and \mathbf{f} , the vector of aerodynamic forces depending on the time t . Damping is neglected in the present model. The stiffness and mass matrices are computed using the Heterosis finite element,¹⁰ which represents a discretization of the Mindlin plate differential equations.

Assuming incompressible linear unsteady aerodynamics and transforming the equations of motion to the frequency domain gives the eigenvalue problem

$$[p^2M + K - qA(p)]\tilde{\mathbf{v}} = 0 \quad (2)$$

where A denotes the matrix of aerodynamic forces, p the eigenvalue, q the dynamic pressure, and $\tilde{\mathbf{v}}$ the eigenvector, meaning that the deformations are of the form

$$\mathbf{v} = \tilde{\mathbf{v}}e^{i\omega t} \quad (3)$$

Following standard procedure,¹¹ the lowest free-vibration frequencies and corresponding eigenmodes are used to define a smaller subspace of size R^m , with m denoting the number of eigenmodes used to define the subspace. Assuming that the free-vibration eigenvectors are normalized so that the generalized mass is 1, the nonlinear eigenvalue problem becomes

$$[p^2I + \Omega^2 - q\hat{A}(p)]\hat{\mathbf{v}} = 0 \quad (4)$$

where Ω^2 is diagonal with the m smallest free-vibration eigenvalues ω_i^2 on the diagonal, and \hat{A} is the $m \times m$ matrix of generalized aerodynamic forces.

It is also convenient to introduce the nondimensional eigenvalue $\hat{p} = pb/u$, with b denoting the semichord of the wing. The imaginary part of \hat{p} is the nondimensional reduced frequency that is usually denoted by $k = \omega b/u$, where ω is the frequency of vibration. A further simplification used is to assume that \hat{A} only depends on the reduced frequency, giving

$$\left[\frac{\rho b^2}{2} \hat{A}(\text{Im } \hat{p}) - \left(\frac{b}{u} \right)^2 \Omega^2 - \hat{p}^2 I \right] \hat{\mathbf{v}} = 0 \quad (5)$$

The nonlinear eigenvalue problem is solved for given values of ρ and u , representing a flight condition. \hat{A} is computed using the doublet-lattice method.¹²

The eigenvalues \hat{p} are found for each flight condition using a modified version of the so-called p - k method¹³ with somewhat better convergence properties. The structure is considered stable for the flight condition if all of the m eigenvalues \hat{p} have a negative real part.

A 16×8 mesh of panels for the full-span wing was used for the discretization of the aerodynamic loads and a 12×6 mesh of finite elements was used for the structural properties of the semispan wing. The size of the modal subspace was chosen to be $m = 16$.

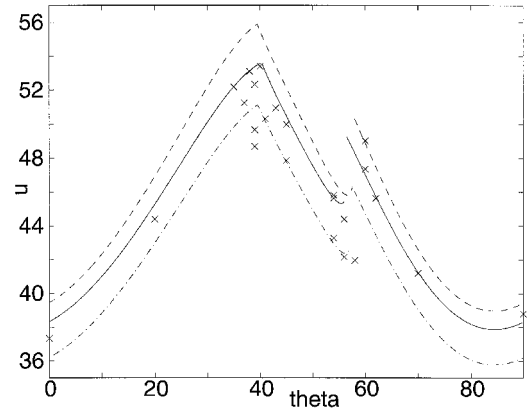


Fig. 2 Critical flutter speed (m/s) vs laminate angle θ .

The three lines in Fig. 2 shows the predicted critical flutter speed as a function of laminate orientation θ for the three different sets of material properties given in Table 1. The thickest plate gives the highest flutter speed.

All three curves share the same general behavior. Each curve can be divided into three regions. The flutter mode below $\theta = 39$ deg corresponds to a bending-torsion mode. At $\theta = 39$ deg there is a change of critical mode resulting in the peak (with discontinuous derivative), and for $39 \text{ deg} < \theta < 57 \text{ deg}$ the flutter mode is a trailing-edge vibration. Another type of transition between flutter modes occurs at $\theta = 57$ deg. This behavior, resulting in a discontinuity, corresponds to a change of critical mode where the two modes are unstable for different airspeeds. Above $\theta = 57$ deg, the eigenvector again corresponds to a bending-torsion mode.

Flutter Speed vs Laminate Orientation

A series of flutter calculations and experiments, conducted at the Royal Institute of Technology, were performed to investigate the correlation between experimental and numerical results. The markers (\times) in Fig. 2 represent the experimental results. Generally, the predictions show good correlation to the experiments. The different eigenmodes discussed earlier were in most cases also qualitatively distinguishable in the experiments.

The main uncertainty in the present model problem relates to the variation in material properties. As can be seen in Fig. 2, the experimental results do not always fall between the two predicted curves representing the upper and lower bound on material properties. However, the magnitude of the difference between the two predicted flutter speeds does surprisingly well correspond to the variation in experimental flutter speed for a given value of θ .

Optimal Design

The purpose of this section is to demonstrate that it may be necessary to change the formulation of the optimal design problem to obtain a design that is stable for a given flight condition not only in the theoretical model but also experimentally. The orientation of the composite material is now considered fixed, at $\theta = 45$ deg, for a wing of the planform shown in Fig. 1. The design problem consists of finding the minimum size and distribution of small masses such that the wing is stable for airspeeds significantly higher than the flutter speed of the bare composite wing.

The optimal design problem of finding the size of additional masses that ensures a stable wing for a given airspeed is posed as the nonlinear optimization problem

$$\min_{w_j} w_0 + \sum_{j=1}^n w_j \quad (6)$$

Table 2 Results from design optimization compared with experimental results

Required speed u , m/s	δ	Total weight, g	w_4 , g	w_5 , g	u_{pred} , m/s	u_{exp} , m/s	u_{diff} , %
—	0	335.6	0	0	47.8	47.8	1.5
55	0	351.1	3.31	12.18	55.0	50.8	7.9
60	0	368.3	4.02	28.72	60.0	51.7	14.9
60	0.001	369.8	5.12	29.07	60.2	53.5	11.8
60	0.01	385.1	17.77	31.74	62.5	61.0	2.4

$$\text{Re } \hat{p}_i(w_j, u) + \delta \leq 0, \quad i = 1, \dots, n_p \quad (7)$$

$$0 \leq w_j, \quad j = 1, \dots, n \quad (8)$$

where w_0 denotes the weight of the bare wing; $\mathbf{w} = (w_1, \dots, w_n)$ is the vector of concentrated masses; and \hat{p}_i denotes the eigenvalues obtained by solving the nonlinear eigenvalue problem for different values of the airspeed. The problem formulation also allows the use of a stability margin $\delta > 0$ that would require the eigenvalues to have a strictly negative real part.

The nonlinear programming problem defined by Eqs. (6–8) is solved using the method of Svanberg¹⁴ and the derivatives of the constraint functions [Eq. (7)] are derived as described in Ref. 6.

The flutter speed of the bare wing was experimentally found to be 47.8 m/s. Numerical calculation resulted in a flutter speed of 47.8 m/s as shown in Fig. 2.

The 12 weights used for mass balancing were equally spaced, six along the leading edge and six along the trailing edge. The weights were numerically modeled as point masses and were experimentally achieved by bonded streamlined lead weights. The optimal design problem [Eqs. (6–8)] involves finding the optimal values of the 12 different weights w_j subject to the stability constraints. The stability constraints were enforced for two different sets of airspeeds; namely, $u = (50, 50.5, 51, \dots, 55)$ m/s and $u = (55, 55.5, 56, \dots, 60)$ m/s. The stability margin $\delta = 0$ was used for the lower airspeed and three different stability margins, $\delta = (0, 0.001, 0.01)$, were used for the higher airspeed. The initial values for solving the optimal design problem was chosen to be zero for all weights corresponding to an infeasible initial design.

The results from the solution of the optimal design problem for the different cases are given in Table 2. Only variables w_j with nonzero optimal values are shown.

It is an interesting feature of the optimal solution that only two variables are nonzero in all cases. The predicted speed, u_{pred} , obtained using the numerical method is somewhat higher than the required speed when $\delta > 0$, because this forces all eigenvalues to be placed the distance δ from the imaginary axis in a root locus plot.

Conclusions

The use of the doublet-lattice method for unsteady subsonic aerodynamics combined with linear elastic finite element structural analysis gives an aeroelastic analysis capability with remarkable accuracy. The simplifying assumptions in the flow model are quite significant, but for the present configuration accurate aerodynamic loads can be calculated. The main uncertainty is because of the variation in material properties. Even though apparently high-quality laminates were used, small variations in thickness have a significant effect on the flutter speed. The influence from internal structural damping and wind-tunnel boundaries appears to have a much smaller effect in the present case.

It was clearly demonstrated that design optimization using the current analysis methods is possible, but stringent quality control is needed if predicted performance is to be realized in practice. The use of optimal design methods for mass balancing clearly demonstrates that using an overly simplistic opti-

mization formulation such as given by Eqs. (6–8) with $\delta = 0$ may result in an optimal design that is of little use in practice. However, if the optimization model allows uncertainties in the aerodynamic and structural model, it is possible to use optimal design. The proposed modified problem formulation [Eqs. (6–8)] with $\delta > 0$ was successful here, but is most likely not the best way to achieve an optimal design with performance that can be experimentally verified.

Acknowledgment

This project was supported by the National Program for Aeronautics Research.

References

- ¹Ashley, H., "On Making Things the Best: Aeronautical Uses of Optimization," *Journal of Aircraft*, Vol. 19, No. 1, 1982, pp. 5–28.
- ²Haftka, R. T., and Yates, E. C., Jr., "Repetitive Flutter Calculations in Structural Design," *Journal of Aircraft*, Vol. 13, No. 7, 1976, pp. 454–461.
- ³Wilkinson, K., Markowitz, J., Lerner, E., George, D., and Batill, S. M., "FASTOP: A Flutter and Strength Optimization Program for Lifting-Surface Structures," *Journal of Aircraft*, Vol. 14, No. 6, 1977, pp. 581–587.
- ⁴Shirk, M. H., Hertz, T. H., and Weisshaar, T. A., "Aeroelastic Tailoring—Theory, Practice, and Promise," *Journal of Aircraft*, Vol. 23, No. 1, 1986, pp. 6–18.
- ⁵Gutkowski, W., Mahrenholtz, O., and Pyrz, M., "Minimum Weight Design of Structures Under Nonconservative Forces," *Lecture Notes of the NATO Advanced Study Institute on Optimization of Large Structural Systems*, edited by G. I. N. Rozvany, Vol. 2, Kluwer, Dordrecht, The Netherlands, 1991, pp. 270–285.
- ⁶Ringertz, U. T., "On Structural Optimization with Aeroelasticity Constraints," *Structural Optimization*, Vol. 8, No. 1, 1994, pp. 16–23.
- ⁷Seyranian, A. P., "Sensitivity Analysis of Multiple Eigenvalues," Dept. of Solid Mechanics, Technical Univ. of Denmark, The Danish Center for Applied Mathematics and Mechanics, Rept. 431, Lyngby, Denmark, 1991.
- ⁸Frederiksen, P. S., "Identification of Material Properties in Anisotropic Plates—A Combined Numerical/Experimental Method," Dept. of Solid Mechanics, Technical Univ. of Denmark, The Danish Center for Applied Mathematics and Mechanics, Rept. S 60, Lyngby, Denmark, 1992.
- ⁹Frederiksen, P. S., "Application of an Improved Model for the Identification of Material Parameters," Dept. of Solid Mechanics, Technical Univ. of Denmark, The Danish Center for Applied Mathematics and Mechanics, Rept. 531, Lyngby, Denmark, 1996.
- ¹⁰Hughes, T. J. R., *The Finite Element Method: Linear Static and Dynamic Finite Element Analysis*, Prentice-Hall, Englewood Cliffs, NJ, 1987.
- ¹¹Dowell, E. H., Curtiss, H. C., Scanlan, R. H., and Sisto, F. A. *Modern Course in Aeroelasticity*. Kluwer, Dordrecht, The Netherlands, 1989.
- ¹²Albano, E., and Rodden, W. P., "A Doublet-Lattice Method for Calculating Lift Distributions on Oscillating Surfaces in Subsonic Flows," *AIAA Journal*, Vol. 7, No. 2, 1969, pp. 279–285.
- ¹³Bäck, P., and Ringertz, U. T., "On the Convergence of Methods for Nonlinear Eigenvalue Problems," Dept. of Aeronautics, Royal Inst. of Technology, TR 96-31, Stockholm, Sweden, 1996.
- ¹⁴Svanberg, K., "The Method of Moving Asymptotes (MMA) with Some Extensions," *Optimization of Large Structural Systems*, edited by G. I. N. Rozvany, Vol. 1, Kluwer, Dordrecht, The Netherlands, 1993, pp. 555–566.